

Nucleosynthesis: Stellar and Solar Abundances and Atomic Data

John J. Cowan,¹ James E. Lawler,² Christopher Sneden,³ E. A. Den Hartog,²
and Jason Collier¹

ABSTRACT

Abundance observations indicate the presence of often surprisingly large amounts of neutron capture (*i.e.*, *s*- and *r*-process) elements in old Galactic halo and globular cluster stars. These observations provide insight into the nature of the earliest generations of stars in the Galaxy – the progenitors of the halo stars – responsible for neutron-capture synthesis. Comparisons of abundance trends can be used to understand the chemical evolution of the Galaxy and the nature of heavy element nucleosynthesis. In addition age determinations, based upon long-lived radioactive nuclei abundances, can now be obtained. These stellar abundance determinations depend critically upon atomic data. Improved laboratory transition probabilities have been recently obtained for a number of elements. These new *gf* values have been used to greatly refine the abundances of neutron-capture elemental abundances in the solar photosphere and in very metal-poor Galactic halo stars. The newly determined stellar abundances are surprisingly consistent with a (relative) Solar System *r*-process pattern, and are also consistent with abundance predictions expected from such neutron-capture nucleosynthesis.

1. Stellar Abundances and New Atomic Data

Abundance studies of heavy elements and isotopes in Galactic halo stars are providing important clues and insights into the nature of, and sites for, nucleosynthesis early in the history of the Galaxy (Sneden & Cowan 2003; Cowan & Thielemann 2004; Cowan & Sneden

¹Homer L. Dodge Department of Physics and Astronomy, University of Oklahoma, Norman, OK 73019; cowan@nhn.ou.edu, collier@nhn.ou.edu

²Department of Physics, University of Wisconsin, Madison, Madison, WI 53706; jelawler@wisc.edu, ead-enhar@wisc.edu

³Department of Astronomy and McDonald Observatory, University of Texas, Austin, Texas 78712; chris@verdi.as.utexas.edu

2006). Observations of heavy neutron-capture elements (*i.e.*, those produced in the slow (*s*) or rapid (*r*)-process) in both old (low iron, or metallicity) stars and younger (more metal-rich) stars are also providing clear indications of the nature of the Galactic chemical evolution. In addition the detection of the long-lived radioactive *n*-capture elements, such as thorium and uranium, are allowing direct age determinations for the oldest stars in the Galaxy - thus, providing lower limits on both the age of the Galaxy and the Universe.

All of these abundance determinations and studies depend critically upon atomic data, particularly transition probabilities. During the past few years there have been dramatic improvements in the experimental determinations of these transition probabilities for a number of rare earth elements: these include improved laboratory values for the elements Ce (Palmeri et al. 2000), Nd (Den Hartog et al. 2003), Ho (Lawler et al. 2004), Pt (Den Hartog et al. 2005), and Sm (Lawler et al. 2006). New values for the element Gd have also recently been obtained (Den Hartog et al. 2006), but Gd abundances in the current paper do not reflect these new data. These improved data sets have been employed to determine elemental abundances in three metal-poor Galactic halo stars. In addition new (refined) solar photospheric abundances have been obtained for Nd, Ho and Sm - this was not possible, however, for Pt. We show in Figure 1 the abundances from Ba-Er (normalized at the *r*-process element Eu) in CS 22892-052 (Snedden et al. 2003), BD +17°3248 (Cowan et al. 2002), HD 115444 (Westin et al. 2000) and the Sun (Lodders 2003). We focus in the left panel on abundance determinations for Nd, Sm and Ho in these four stars based upon published atomic data. The abundances for those same three elements, employing the newer laboratory atomic data, is shown in the right panel of this figure. It is clear, that as a result of employing the new atomic data, the star-to-star scatter among the three metal-poor Galactic halo stars is markedly reduced, and there is good agreement between the elemental values in these stars and the solar system *r*-process value (indicated by the horizontal line).

2. Discussion

Employing the new atomic data, we have updated several of the abundance values from Sneden et al. (2003) for CS 22892-052. We show those values in Figure 2 (top panel) compared to an *s*-only (dashed line) and an *r*-only (solid line) solar system elemental abundance curve. These solar system elemental abundance curves from Simmerer et al. (2004) are the sums of individual isotopic contributions from the *s* and *r*-process and are tabulated in table 1. Using the so called “classical model” approximation in conjunction with measured neutron capture cross-sections, the individual *s*-process contributions are first determined. Subtracting these *s*-process isotopic contributions from the total solar abundances predicts the residual *r*-process contributions. These individual *s*- and *r*-process isotopic solar system abundances (based upon the Si = 10⁶ scale) that are listed in table 1, are derived from the work of Käppeler et al. 1989, Wisshak et al. 1998 and O’Brien et al. 2003, and can be used for future isotopic studies.

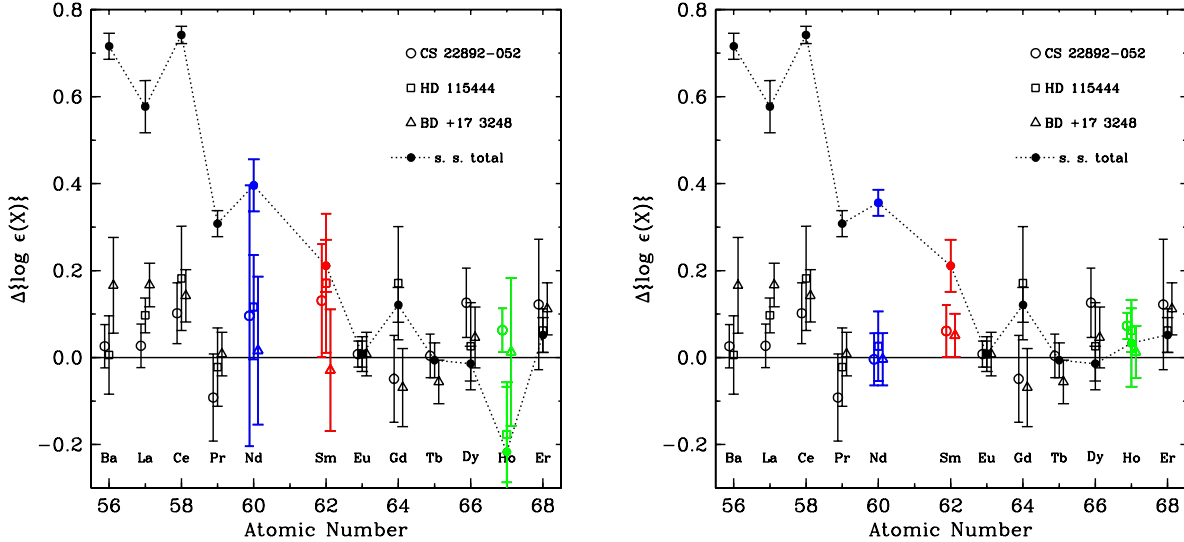


Fig. 1.— (left) Abundance values (scaled at the element Eu) for selected elements in the stars CS 22892-052 (open circles), HD 115444 (squares), BD +17°3248 (triangles) and the Sun (filled circles), based upon previously published atomic data. (right) Newly derived abundance values based upon recent experimental lab data (after Lawler et al. 2006).

It is clear in both the top and bottom panels of Figure 2 that the abundances of the stable elements Ba and above are consistent with the scaled solar system elemental r -process distribution. This agreement has been seen in other r -process-rich stars and strongly suggests that the r -process is robust over the history of the Galaxy. It further demonstrates that early in the history of the Galaxy, all of the n -capture elements were synthesized in the r -process, and not the s -process. Additional comparisons in the figure, however, suggest the lighter elements do not fall on this same curve that fits the heavier n -capture elements. The upper limit on Ge, for example, falls far below the scaled solar system r -process curve. Recent analyses of this element indicates its abundance is tied to the iron level in metal-poor halo stars (Cowan et al. 2005), and thus suggests Ge synthesis in some type of charged-particle reactions, or other primary process, in massive stars and supernovae in the early Galaxy (see discussion in Cowan & Sneden 2006). We also note that the abundances of the n -capture elements from $Z = 40$ –50 in CS 22892-052, in general, fall below the solar r -process curve. This has been interpreted as suggesting perhaps a second r -process synthesis site in nature (see discussion in Kratz et al. 2006 and Cowan & Sneden 2006). Interestingly, new abundances studies of the star HD 221170 show better agreement with the scaled solar system curve for the elements from $Z = 40$ –50 than CS 22892-052 does (Ivans et al. 2006).

In spite of the good overall match between the scaled-solar r -process abundances and

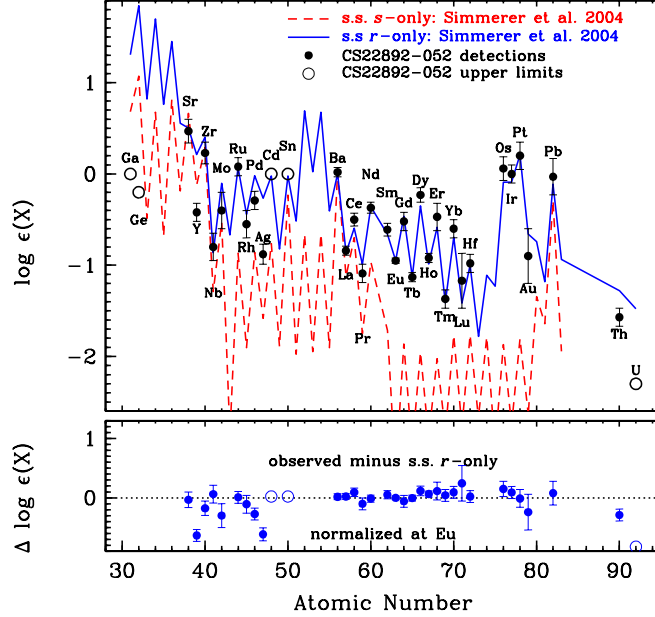


Fig. 2.— (top) Abundance values for CS 22892-052 compared to a scaled solar system *s*-process (dashed line) and *r*-process distribution (solid line, Simmerer et al. 2004). (bottom) Differences between observed abundances in CS 22892-052 and the scaled solar system *r*-process abundances (after Cowan & Sneden 2006).

those of very metal-poor stars, some small deviations are becoming apparent, as shown in Figures 1 and 2. The increasingly accurate stellar abundance determinations, resulting in large part from the more accurate laboratory atomic data, are helping to constrain, and ultimately could predict, the actual values of the solar system *r*-process abundances. Thus, the current differences might suggest that some of those solar system *r*-process elemental predictions need to be reassessed. Recall that the elemental *r*-process curve is based upon the isotopic *r*-process residuals, resulting from the subtraction of the *s*-process isotopic contributions from the total solar system abundances. Thus, a reanalysis of some of the *s*-process contributions, and new neutron-capture cross sections measurements, might be in order.

3. Conclusions

Abundance observations of metal-poor (very old) Galactic halo stars indicate the presence of *n*-capture elements. New laboratory atomic data is dramatically reducing the stellar abundance uncertainties in these stars and increasingly improving the Solar System abun-

dances. Recently determined abundances, based upon the new laboratory data, indicate that the elemental patterns in the old halo stars are consistent with each other and with a scaled solar system r -process abundance distribution – demonstrating that all of these elements (even s -process ones like Ba) were synthesized in the r -process early in the history of the Galaxy. These more accurate abundance determinations, based upon more precise laboratory atomic data, might be employed to constrain predictions for the solar system r -process abundances. In the future additional (and improved) lab data will have implications for a number of synthesis studies, including providing evidence regarding the possibility of two astrophysical r -process sites. Such new experimental data will also help in understanding the Galactic chemical evolution of the elements, and could have an impact on chronometric age estimates of the Galaxy and the Universe. New stellar and atomic data in both the UV and IR wavelength regimes may also allow the detection of never before seen elements in these stars, and will aid in new determinations of isotopic abundance mixtures for elements such as Sm.

We thank our colleagues for valuable insights and contributions. This work has been supported in part by NSF grants AST 03-07279 (J.J.C.), AST 05-06324 (J.E.L.), AST 03-07495 (C.S.), and by STScI.

REFERENCES

- Cowan, J. J., et al. 2002, ApJ, 572, 861
Cowan, J. J., et al. 2005, ApJ, 627, 238
Cowan, J. J., & Sneden, C. 2006, Nature, in press
Cowan, J. J., & Thielemann, F.-K., 2004, Phys. Today, 57, 47
Den Hartog, E. A., Lawler, J. E., Sneden, C., & Cowan, J. J. 2003, ApJS, 148, 543
Den Hartog, E. A., Herd, T. M., Lawler, J. E., Sneden, C., Cowan, J. J., & Beers, T. C. 2005, ApJ, in press
Den Hartog, E. A., Lawler, J. E., Sneden, C., & Cowan, J. J. 2006, ApJ, to be submitted
Ivans, I. I., et al. 2006, ApJ, in press
Käppeler, F., Beer, H. & Wisshak, K. 1989, Rep. Prog. Phys., 52, 945
Kratz, K.-L., Farouqi, K., Pfeiffer, B., Truran, J. W., Sneden, C., & Cowan, J. J. 2006, ApJ, in preparation
Lawler, J. E., Den Hartog, E. A., Sneden, C., & Cowan, J. J. 2005, ApJ, in press
Lawler, J. E., Sneden, C., & Cowan, J. J. 2004, ApJ, 604, 850
Lodders, K. 2003, ApJ, 591, 1220
O’Brien, S., et al. 2003, Pys. Rev. C, 68, 035801
Palmeri, P., Quinet, P., Wyart, J.-F., & Biéumont, E. 2000, Physica Scripta, 61, 323
Simmerer, J., Sneden, C., Cowan, J. J., Collier, J., Woolf, V. M., & Lawler, J. E. 2004, ApJ, 617, 1091
Sneden, C., et al. 2003, ApJ, 591, 936

Sneden, C., & Cowan, J. J. 2003, *Science*, 299, 70

Westin, J., Sneden, C., Gustafsson, B., & Cowan, J.J. 2000, *ApJ*, 530, 783

Wisshak, K., Voss, F., Käppeler, F., Kazakov, L., & Reffo, G. 1998, *Phys. Rev. C*, 57, 391

Table 1. *s*- AND *r*-PROCESS ISOTOPIC SOLAR SYSTEM ABUNDANCES

Element	Z	Isotope	N[s]	N[r]	Element	Z	Isotope	N[s]	N[r]
Ga	31	69	11.137	11.600	Pd	46	104	0.165	0.000
		71	10.413	4.700			105	0.040	0.269
Ge	32	70	15.000	0.000			106	0.186	0.193
		72	18.323	14.000			108	0.226	0.145
		73	3.531	5.670			110	0.000	0.163
		74	15.733	27.300	Ag	47	107	0.058	0.239
		76	0.000	9.200			109	0.059	0.196
As	33	75	1.456	5.330	Cd	48	110	0.178	0.000
Se	34	76	4.656	0.000			111	0.042	0.165
		77	1.679	3.040	112	0.198	0.196		
		78	7.402	7.210	113	0.060	0.139		
		80	7.446	24.300	114	0.287	0.140		
		82	0.000	5.710	116	0.000	0.121		
		79	0.450	0.000	In	49	115	0.057	0.121
81	0.479	4.640	Sn	50			116	0.511	0.000
Kr	36	80			1.021	0.000	117	0.146	0.128
		82	6.207	0.000	118	0.706	0.137		
		83	1.989	3.750	119	0.155	0.065		
		84	10.575	18.000	120	1.099	0.078		
		86	9.481	0.930	122	0.000	0.154		
Rb	37	85	0.690	2.790			124	0.000	0.199
		87	2.214	0.100	Sb	51	121	0.047	0.113
Sr	38	86	2.111	0.000			123	0.000	0.132
		87	1.443	0.000	Te	52	122	0.133	0.000
88	16.986	2.550	123	0.047			0.000		
Y	39	89	3.344	1.310			124	0.248	0.000
		90	4.529	0.990			125	0.088	0.267
Zr	40	91	1.158	0.040			126	0.450	0.525
		92	1.289	0.540	128	0.000	1.526		
		94	1.687	0.170	130	0.000	1.634		
		96	0.000	0.300	I	53	127	0.050	0.851
		95	0.229	0.110			128	0.126	0.000
Nb	41	95	0.189	0.213	Xe	54	129	0.066	1.240
		96	0.475	0.000			130	0.199	0.000
Mo	42	97	0.156	0.087	131	0.087	0.954		
		98	0.514	0.093	132	0.498	0.800		
		100	0.000	0.242	134	0.000	0.449		
		99	0.006	0.172	136	0.000	0.373		
		99	0.049	0.000	Cs	55	133	0.056	0.315
100	0.242	0.000	Ba	56			134	0.178	0.000
101	0.050	0.266			135	0.068	0.298		
102	0.261	0.327			136	0.500	0.000		
104	0.000	0.348			137	0.372	0.283		
103	0.055	0.289			138	3.546	0.225		
Rh	45	103	0.055	0.289					
La	57	139	0.337	0.110	Lu	71	175	0.006	0.031
Ce	58	140	0.894	0.089			176	0.002	0.000
		142	0.000	0.115	Hf	72	176	0.008	0.000
Pr	59	141	0.079	0.082			177	0.005	0.024
		Nd	60	142	0.227	0.000	178	0.021	0.022
143	0.037			0.065	179	0.007	0.015		
144	0.105			0.094	180	0.035	0.020		
145	0.020			0.049	Ta	73	181	0.009	0.013

Table 1—Continued

Element	Z	Isotope	N[s]	N[r]	Element	Z	Isotope	N[s]	N[r]
		146	0.091	0.053	W	74	182	0.024	0.012
		148	0.004	0.044			183	0.013	0.007
		150	0.000	0.047			184	0.029	0.013
Sm	62	147	0.003	0.031			186	0.006	0.031
		148	0.038	0.000	Re	75	185	0.004	0.014
		149	0.005	0.031			187	0.001	0.033
		150	0.022	0.000	Os	76	186	0.012	0.000
		152	0.018	0.053			187	0.006	0.000
		154	0.000	0.059			188	0.016	0.079
Eu	63	151	0.000	0.042			189	0.004	0.111
		153	0.002	0.048			190	0.021	0.168
Gd	64	152	0.001	0.000			192	0.001	0.293
		154	0.009	0.000	Ir	77	191	0.005	0.241
		155	0.003	0.045			193	0.003	0.408
		156	0.015	0.055	Pt	78	192	0.010	0.000
		157	0.007	0.046			194	0.020	0.431
		158	0.027	0.058			195	0.006	0.457
		160	0.000	0.072			196	0.035	0.312
Tb	65	159	0.004	0.060			198	0.000	0.099
Dy	66	160	0.009	0.000	Au	79	197	0.010	0.176
		161	0.004	0.075	Hg	80	198	0.035	0.000
		162	0.016	0.101			199	0.016	0.043
		163	0.002	0.093			200	0.051	0.030
		164	0.018	0.091			201	0.020	0.027
Ho	67	165	0.006	0.083			202	0.079	0.026
Er	68	164	0.004	0.000			204	0.000	0.020
		166	0.012	0.072	Tl	81	203	0.042	0.012
		167	0.005	0.053			205	0.060	0.041
		168	0.020	0.047	Pb	82	204	0.057	0.000
		170	0.001	0.037			206	0.326	0.223
Tm	69	169	0.006	0.031			207	0.313	0.280
Yb	70	170	0.006	0.000			208	1.587	0.118
		171	0.004	0.029	Bi	83	209	0.051	0.093
		172	0.018	0.036	Th	90	232	0.000	0.042
		173	0.008	0.031	U	92	235	0.000	0.006
		174	0.040	0.037			238	0.000	0.020
		176	0.000	0.030					